

# Digital Data Analysis Techniques for Extraction of Slosh Model Parameters

J. F. Unruh\*, D. D. Kana†, F. T. Dodge‡, and T. A. Fey§  
*Southwest Research Institute, San Antonio, Texas*

Modern digital acquisition and modal analysis procedures are applied to the slosh model parameter extraction problem with considerable success. After appropriate data conditioning to remove the tank rigid and liquid rigid mass from the spectral data, the slosh peaks are "circle fit" to obtain estimates of the pendulum's masses, damping, and pivot arm locations. Circle fitting the data about the slosh peak does not require data acquisition at precisely the slosh resonance; therefore, the time for data acquisition and the probability of error in the model parameter estimates are greatly reduced. Equations of motion for the slosh pendulum model are reviewed along with the analytical procedures associated with circle fitting the data in the region of the slosh resonance. The experimental setup of a 1:4.85 scale model Centaur Booster fuel tank is described along with the data acquisition procedures used to obtain forced harmonic response slosh data. Several examples are given to demonstrate the accuracy of the circle fitting procedures for obtaining slosh model parameters by direct comparison of experimental data to model generated response data.

## Nomenclature

$b$	= separation distance between applied forces
$c_\alpha$	= pendulum rotational damper coefficient
$d$	= tank diameter
$f_\ell$	= lower force applied to tank
$f_p$	= pendulum reaction force
$f_u$	= upper force applied to tank
$g$	= gravity
$h$	= in general, distance from tank reference axis to system mass or slosh pendulum pivot or liquid depth
$i$	= index or imaginary number $\sqrt{-1}$
$j, k$	= indices
$\ell$	= slosh pendulum arm
$m$	= in general, a system mass
$\ddot{x}$	= tank lateral acceleration
$y$	= real part of $(\omega/\bar{W}^k)$ , see Eq. 20
$A, B, D$	= constants defined in Eq. 21
$F$	= in general, a force
$M(\omega)$	= tank apparent mass moment
$M_p$	= pendulum reaction moment
$N$	= number of slosh resonances
$R$	= number of data points about slosh resonance
$T$	= tension in slosh pendulum arm
$W(\omega)$	= tank apparent mass
$\alpha$	= pendulum rotation
$\beta$	= pendulum critical damping ratio
$\phi$	= tank pitch
$\epsilon$	= small frequency increment
$\omega$	= circular frequency
$\xi$	= liquid eigenvalues

## Subscript

0	= liquid rigid mass
---	---------------------

## I. Introduction

THE development of simplified linear dynamic models of fluid sloshing in spacecraft fuel tanks is an important task in assessing the dynamic response of the spacecraft system. Fuel slosh has been responsible for excessive spacecraft excitation, which results in greatly reduced lifetime due to excessive fuel expenditure for spacecraft stabilization. Dynamic characterization of the fuel slosh phenomenon in terms of a series of discrete pendulum oscillators is particularly well suited to the variable gravity environment experienced by spacecraft. Extraction of accurate pendulum slosh model parameters from ground scale model tests is a difficult task due to the low damped, low frequency characteristics of the slosh phenomena.

The Centaur G-Prime and G propellant tanks are currently scheduled for launch of the Ulysses, Galileo, and other satellites from shuttle orbit. Earlier versions of these tanks have been used for other applications in the past, and liquid slosh was addressed by the particular configuration/application. However, current configurations include new tank dimensions and baffle designs, whose slosh characteristics have not been evaluated. Therefore, a new series of combined experimental and analytical studies were conducted to develop parameters for constructing linear analytical slosh models for the new tank configurations. An approximately  $\frac{1}{5}$  scale model of the propellant tank was used for the system identification study.

The use of equivalent mechanical models to represent the dynamics of sloshing in system studies has a long history.<sup>1</sup> The models have ranged from simple one-pendulum models<sup>2</sup> to complete models that even represent nonlinear effects such as rotary sloshing. Equivalent mechanical models have also proved useful to represent low-g sloshing.<sup>3</sup> All the models are based upon the observation that the forces and moments exerted on a tank as predicted by ideal, irrotational, potential flow are similar in form to those predicted by a system of pendulums (or masses and springs). For example, the fluid dynamics force given by the linearized potential flow solution for sloshing in an upright cylindrical tank excited by simple-

Submitted Feb. 4, 1985; presented as Paper 85-0813 at the AIAA/ASME/ASCE/AHS 26th Structures, Structural Dynamics and Materials Conference, Orlando, FL, April 15-17, 1985; revision received June 6, 1985. Copyright © American Institute of Aeronautics and Astronautics, Inc., 1985. All rights reserved.

\*Staff Engineer, Engineering Mechanics. Senior Member AIAA.

†Institute Engineer, Engineering Mechanics. Associate Fellow AIAA.

‡Institute Engineer, Mechanical Sciences. Associate Fellow AIAA.

§Research Engineer, Engineering Mechanics.

harmonic translation  $x$  and pitching  $\phi$  is

$$F = -m_{\text{liquid}} \ddot{x} \left\{ 1 + \sum_{n=1}^{\infty} \frac{(\omega/\omega_n)^2 \tanh(2\xi_n h/d)}{(\xi_n h/d)(\xi_n^2 - 1)[1 - (\omega/\omega_n)^2]} \right\} \\ - m_{\text{liquid}} \ddot{\phi} \sum_{n=1}^{\infty} \frac{\tanh(2\xi_n h/d)}{(\xi_n h/d)(\xi_n^2 - 1)} \\ \times \left\{ \frac{\frac{h}{2}(\omega/\omega_n)^2 \left[ 1 - \frac{2d}{\xi_n h} \tanh(\xi_n h/d) \right] + \frac{g}{\omega_n^2}}{1 - (\omega/\omega_n)^2} \right\} \quad (1a)$$

where  $\omega$  is the frequency of the simple harmonic input motion and  $\omega_n$  is the natural frequency of the  $n$ th slosh mode

$$\omega_n = \left[ \frac{2g\xi_n \tanh(2\xi_n h/d)}{d} \right]^{\frac{1}{2}} \quad (1b)$$

Here  $\xi_n$  are the eigenvalues of the problem ( $\xi_1 = 1.841$ ,  $\xi_2 = 5.331$ , etc.). The liquid depth is  $h$  and the tank diameter is  $d$ . The force exerted on the same tank by a system of pendulums, each with a pendulum mass  $m_n$ , and one mass  $m_0$  rigidly fixed to the tank is

$$F = -m_{\text{total}} \ddot{x} \left\{ 1 + \sum_{n=1}^{\infty} \left( \frac{m_n}{m_{\text{total}}} \right) \left[ \frac{(\omega/\omega_n)^2}{1 - (\omega/\omega_n)^2} \right] \right\} \\ - m_{\text{total}} \ddot{\phi} \sum_{n=1}^{\infty} \left( \frac{m_n}{m_{\text{total}}} \right) \left[ \frac{h_n(\omega/\omega_n)^2 + g/\omega_n^2}{1 - (\omega/\omega_n)^2} \right] \quad (2)$$

By comparing Eqs. (1) and (2), it can be seen that the mechanical model of pendulums will duplicate exactly the forces predicted by the potential flow if 1) the total mass of all the pendulums and the rigidly attached mass is taken equal to the total liquid mass (which is also a requirement to duplicate the static loads), 2) the pendulum masses are chosen in accordance with

$$\frac{m_n}{m_{\text{total}}} = \frac{\tanh(2\xi_n h/d)}{(\xi_n h/d)(\xi_n^2 - 1)} \quad (3a)$$

and 3) the vertical locations of the pendulum hinge points with respect to the center of the liquid mass are taken as

$$\frac{h_n}{h} = \left[ 1/2 - (d/\xi_n h) \tanh(\xi_n h/d) \right] \quad (3b)$$

The magnitude and location of the rigidly attached mass are determined by requiring the model to have the same center-of-mass location as the liquid.

In any real liquid the sloshing is damped by viscous effects. The damping is readily included in the mechanical model, at least for small damping, by modifying the denominators of Eq. (2); however, the damping factors usually must be determined experimentally.

In tanks that contain baffles, are non-axisymmetric or perhaps undergo nonlinear sloshing, the entire mechanical model must be determined empirically by the use of methods such as are discussed in this article. The theory outlined above remains as the justification for such models, even though there may not be any fluid-dynamics predictions with which to compare the test results.

When the slosh parameters are determined empirically by scale-model testing, as they were in this study, the test program must be conducted in accordance with the requirements of similarity. The most important scaling parameter, for a

geometrically scaled tank, is the Froude number<sup>1</sup> which states that all frequencies, including the slosh resonant frequencies, are scaled in proportion to  $(g/d)^{\frac{1}{2}}$ . A complete dimensional analysis then shows that the model masses are scaled in proportion to the total liquid mass and all length-like dimensions are scaled geometrically. The scaling of damping is more difficult and cannot be accomplished simply by Froude scaling. Reynolds number scaling is also required and this is generally impossible. But previous studies<sup>1</sup> have shown that the viscous damping coefficient for sloshing in a bare-wall tank is roughly proportional to  $(\nu^2/R^3g)^{\frac{1}{4}}$ , where  $\nu$  is the kinematic viscosity of the liquid. This factor can be used to scale-up the measured damping to full-scale, even though viscous effects were not scaled in the tests. Drag-like damping due to baffles, for geometrically scaled baffles and wave heights, generally scales one-to-one in terms of log decrements between model and full-scale,<sup>1</sup> so, again, the full-scale damping can be predicted from model tests. Note that damping is only a governing parameter when resonant sloshing is excited; otherwise, the exact values of the damping coefficients are not critical.

In the sections to follow, the equations of motion for a liquid-filled tank represented as a series of mass pendulums will be developed in a form suitable for parameter identification studies. The data analysis procedures, employing modern modal analysis parameter extraction techniques, will then be developed to extract the equivalent pendulum parameters. A brief description of the G-Prime tank configuration, experimental setup, and data acquisition procedures will then be given along with typical analysis results for a smooth tank and a tank with baffles. Further discussions of the dynamic characteristics of the various G and G-Prime tank configurations are beyond the scope of the present paper, however these results will be published later.

## II. Pendulum Slosh Model

The equations of motion for a liquid filled tank excited laterally with pure translational acceleration are developed from force and moment summations on the tank and pendulum slosh masses. In the following development, only a single slosh mass will be dealt with explicitly, but extension of the equations of motion for multiple slosh masses is straightforward. The liquid filled tank geometry and system masses under consideration are as shown in Fig. 1. The system considers two lateral forces,  $f_u$  and  $f_\ell$ , applied to the tank to produce the pure translational acceleration  $\ddot{x}$ . The tank reference axis is placed along the line of action of the lower force and the center line of the tank. The empty tank mass and height above the reference axis are  $m_T$  and  $h_T$ , respectively. That portion of liquid that remains in contact with the tank and acts as a rigid liquid mass at high frequencies is denoted as  $m_0$  at location  $h_0$  above the reference axis. The pendulum arm, length  $\ell_1$ , of the slosh mass  $m_1$  pivots about a point  $h_1$  above the tank reference axis. The horizontal load applied to the tank due to the slosh mass motion is denoted as  $f_p$  and the moment as  $M_p$ .

A free body diagram of the slosh mass pendulum is shown in Fig. 2 along with the various inertial, centrifugal, damping, and gravity forces acting on the mass during angular motion  $\alpha$ . The tension in the pendulum arm is  $T$  and the pendulum motion is damped via a rotational viscous damper with coefficient  $c_\alpha$ .

A summation of forces acting on the slosh mass in the horizontal direction yields

$$\sum F_H = 0 = m_1 \ddot{x} + \left( \ddot{\alpha} \ell_1 m_1 + \frac{c_\alpha \dot{\alpha}}{\ell_1} \right) \cos \alpha \\ - \dot{\alpha}^2 \ell_1 m_1 \sin \alpha + T \sin \alpha \quad (4a)$$



and

$$M(\omega \gg \omega_N) = m_T h_T + m_0 h_0 \quad (13b)$$

show that the influence of the slosh masses are completely removed at high frequencies. In general, when the system is excited at the  $k$ th slosh resonance

$$W(\omega_k) = m_T + m_0 + \sum_{j=k+1}^N m_j + m_k \left\{ 1 - \frac{i}{2\beta_k} \right\} \quad (14a)$$

and

$$M(\omega_k) = m_T h_T + m_0 h_0 + \sum_{j=k+1}^N m_j h_j + m_k h_k \left\{ 1 - \frac{i}{2\beta_k} \right\} - m_k \ell_k \quad (14b)$$

### III. Data Analysis Procedures

The task to extract the various liquid masses, moment arms, and damping ratios from direct measurement of tank apparent mass  $W(\omega)$  and mass moment  $M(\omega)$  employs the "circle fit" method of parameter extraction for equivalent single degree of freedom systems (Eq. 4). The procedures for conditioning these measurements to isolate the equivalent single degree of freedom system, i.e., a single slosh mode, are as follows. Direct measurement of the empty tank parameters  $m_T$  and  $h_T$  are straightforward; i.e., a linear average of empty tank data taken at various excitation frequencies should yield good estimates of these parameters. The rigid liquid mass  $m_0$  and center of gravity  $h_0$  are obtained via averaging of high frequency measurements using the results given in Eqs. (13a) and (13b), thus,

$$m_0 = W(\omega \gg \omega_N) - m_T \quad (15a)$$

and

$$h_0 = [M(\omega \gg \omega_N) - m_T h_T] / m_0 \quad (15b)$$

The effects of the empty tank and rigid liquid mass are then removed from the measurements as

$$\bar{W}(\omega) = W(\omega) - m_T - m_0 \quad (16a)$$

and

$$\bar{M}(\omega) = M(\omega) - m_T h_T - m_0 h_0 \quad (16b)$$

Consider the system response for well separated resonances in the neighborhood of the  $k$ th slosh resonance where  $\omega_k - \epsilon \leq \omega \leq \omega_k + \epsilon$ , then

$$\begin{aligned} W^k(\omega) &\equiv \lim_{\omega \rightarrow \omega_k} \bar{W}(\omega) \\ &\cong \sum_{j=k+1}^N m_j + m_k \left\{ 1 + \frac{\omega^2}{\omega_k^2 - \omega^2 + i2\beta_k \omega_k \omega} \right\} \end{aligned} \quad (17a)$$

However, when the frequency is within  $\epsilon$  (i.e., within a small frequency increment of the slosh resonant frequency  $\omega_k$ ), then

$$\frac{\omega^2}{\omega_k^2 - \omega^2 + i2\beta_k \omega_k \omega} \gg 1$$

which allows further simplification of Eq. (17a) to form

$$\bar{W}^k(\omega) = W^k(\omega) - \sum_{j=k+1}^N m_j$$

or

$$\bar{W}^k(\omega) = \frac{m_k \omega^2}{\omega_k^2 - \omega^2 + i2\beta_k \omega_k \omega} \quad (17b)$$

Inverting Eq. (17b) and multiplying through by  $\omega$  yields

$$\left( \frac{\omega}{\bar{W}^k(\omega)} \right) = \left( \frac{\omega_k^2}{m_k} \omega^{-1} - \frac{1}{m_k} \omega \right) + i \left( \frac{2\beta_k \omega_k}{m_k} \right) \quad (18)$$

which is a form of the response that can be "circle fit" to yield the  $k$ th slosh mass parameters. Note that a Nyquist plot of  $(\omega/\bar{W}^k)$  is a straight line  $2\beta_k \omega_k/m_k$  above the real axis and the Nyquist plot of  $(\bar{W}^k/\omega)$  is a circle tangent to the real axis with a diameter equal to  $m_k/2\beta_k \omega_k$ . Thus we are performing a circle fit of the data about the apparent resonance point.

For  $R$  data points about the resonance frequency an average of the imaginary part of  $(\omega/\bar{W}^k)$  yields an estimate of the parameter ratio

$$2\beta_k \omega_k / m_k = 1/R \sum_{i=1}^R \text{Im}(\omega / \bar{W}^k) \quad (19)$$

The real part of  $(\omega/\bar{W}^k)$  is written as

$$\text{Re}(\omega / \bar{W}^k) = y = A \omega^{-1} - B \omega \quad (20)$$

where the constants  $A$  and  $B$  equal  $\omega_k^2/m_k$  and  $1/m_k$ , respectively. A least square error fit to  $R$  data points about the resonance frequency results in two coupled equations from which the constants  $A$  and  $B$  are determined as

$$A = \left( \sum_{i=1}^R \omega_i^2 \sum_{i=1}^R y_i \omega_i^{-1} - R \sum_{i=1}^R y_i \omega_i \right) / D \quad (21a)$$

and

$$B = \left( R \sum_{i=1}^R y_i \omega_i^{-1} - \sum_{i=1}^R \omega_i^{-2} \sum_{i=1}^R y_i \omega_i \right) / D \quad (21b)$$

where

$$D = \sum_{i=1}^R \omega_i^{-2} \sum_{i=1}^R \omega_i^2 - R^2 \quad (21c)$$

Estimates of the slosh model parameters are then found as

$$m_k = 1/B,$$

$$\omega_k = (A/B)^{\frac{1}{2}}$$

and

$$\beta_k = \frac{1}{2(AB)^{\frac{1}{2}}} \frac{1}{R} \sum_{i=1}^R \text{Im} \left[ \frac{\omega}{\bar{W}^k} \right] \quad (22)$$

Similar conditioning procedures applied to the tank apparent mass moment data follows direct ratioing of the imaginary parts of the tank mass moment and mass response data to obtain an estimate of the location of the slosh pivot  $h_k$ . The slosh pendulum arm  $\ell_k$  is determined directly from  $\omega_k$  as  $\ell_k = g/\omega_k^2$ .

The above procedures indicate that harmonic data need only be taken around the peaks of the slosh resonances and at the higher frequencies above which measurable slosh occurs in order to extract the model parameters. As can be seen from Eq. (17b), the slosh parameter analysis must begin at the highest slosh resonance so that in turn, the off-loaded slosh masses will be available from previous circle fit analyses.

#### IV. Example Application

##### Tank Configuration

The Centaur G-Prime model consists principally of four major parts: an ellipsoidal LOX dome for the base bulkhead, a conical section attached to the bulkhead, a cylindrical extension, and an ellipsoidal cover (see Fig. 3). The model was molded out of  $\frac{3}{8}$ -in. plexiglass to facilitate viewing and filming of the liquid slosh. Aluminum rings were attached to the plexiglass molded sections for structural support. The model was constructed in sections so portions of the tank could easily be removed to decrease tank weight to give better resolution for data acquisition at the lower liquid levels. Scaled baffles were constructed and attached to the conical section and LOX dome at the base of the model to alter the system natural frequencies and damping. Figure 3 shows the tank in the completely assembled configuration, and oriented for horizontal translation excitation on a pendulum support. The pendulum support frequency was quite low ( $\sim 0.26$  Hz), and therefore it was not necessary to include support resonance effects in the modeling.

##### Experimental Setup

The tank was excited at two points a known distance apart through two strain gage type load cells. The two load cells were attached to a common rigid support which was part of the drive. The drive was provided by a servo-controlled hydraulic actuator. Two strain gage type accelerometers were used to record the tank accelerations in line with the input forces. Comparison of the accelerometers allowed evaluation of pure translation input motion. The actuator displacement was also recorded using a linear variable displacement transducer to insure accurate low frequency recording, below the accurate range of the accelerometers. Tap water, colored to improve contrast for filming, was used as the slosh liquid.

##### Data Acquisition and Reduction

Digital data acquisition was performed on the five data channels—two force signals, two acceleration signals, and one displacement signal. The data channels were signal conditioned, amplified and band pass filtered, prior to digital recording to insure a sufficient signal to noise ratio for accurate

signal recording throughout the frequency range of interest (0.2 to 10 Hz).

The data acquisition and control was carried out via FORTRAN level software resident in a Digital Equipment Corporation PDP 11/23 minicomputer. A CAMAC (Computer Automated Measurement and Control) system [5] provided the electrical hardware and software interfaces from the transducer to the PDP 11/23. CAMAC 3520 12-bit analog to digital interfaces were used to acquire 512 sample points for each data channel. The digitization rate was optimized for the particular frequency of the harmonic drive signal. Immediate fast Fourier transformation (FFT) of the data allowed direct extraction and storage of the phase correlated data.

Each of the slosh resonances were initially identified so that data could be digitally recorded mainly in the area of the resonance points. With low damped, low frequency slosh modes this preliminary process was very tedious and time-consuming. System nonlinearities also aggravated the process, however tank excitation levels were generally maintained sufficiently low to preclude dominant nonlinear response. The data analysis procedures detailed in Sec. III were programmed via FORTRAN on a D.E.C. PDP 11/70 minicomputer to carry out the model parameter extraction and postprocessing operation.

##### Typical Results

Two sets of sample results developed for the Centaur G-Prime tank will now be described. The first set is for the barewall tank at designated liquid level-3, for which the liquid is 1.24 in. below the cylinder-cone intersection. The quiescent liquid surface does not quite clear the LOX dome for this level. A summary of all data is given in Table 1, while plotted results for effective weight are given in Fig. 4 and effective moment are given in Fig. 5. Effective weight in lb is understood to be the product of apparent mass  $[W(\omega)]$  given by Eq. (10)] and standard gravity  $g$ . Similarly, the effective moment in in.-lb is the product of apparent mass moment  $[M(\omega)]$  given by Eq. (11)] and standard gravity  $g$ .

From Table 1 it can be seen that the circle fit data were generated for 3, 5, and 7 points successively about each of the two resonances, and a corresponding plot generated. A least square fit of the experimental data to the generated curve was then computed. For both modes, it can be seen that use of three experimental points provided the smallest least squares error, these data were nearest to the apparent resonance point.

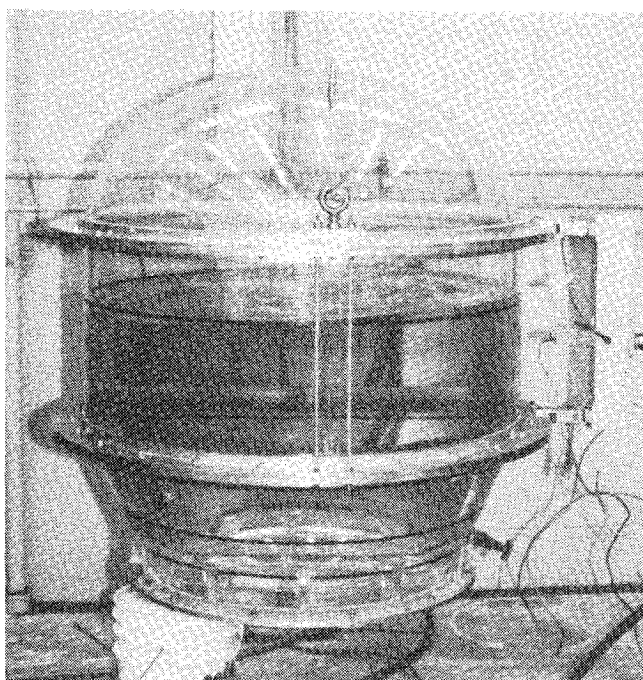


Fig. 3 Scale model G-prime tank.

Table 1 Liquid level 3 smooth tank slosh model parameters

Tank excitation level: 0.0200 in.

Slosh model parameter extraction

Input: Empty tank weight 118.28 lb  
Empty tank c.g. 1.514 in.  
Rigid fluid weight 34.77 lb  
Rigid fluid c.g. 1.815 in.

Slosh resonance data analysis mode no. 2

NPTS	$f_i$ , freq	$\beta_i$ , beta	error	$h_i$ , pivot	$m_i g$ , weight	$\ell_i$ , arm
3	1.5002	0.0103	0.0002	-0.185	14.93	4.344
5	1.5002	0.0085	0.0005	-0.385	15.32	4.345
7	1.4987	0.0070	0.0047	-1.391	15.67	4.353

Slosh resonance data analysis mode no. 1

NPTS	$f_i$ , freq	$\beta_i$ , beta	error	$h_i$ , pivot	$m_i g$ , weight	$\ell_i$ , arm
3	0.6368	0.0062	0.0000	9.363	107.84	24.112
5	0.6361	0.0037	0.0005	9.043	73.31	24.166
7	0.6356	0.0032	0.0006	8.793	67.86	24.199

$\Sigma m_i g = 157.5$  lb, actual liquid  $W_L = 148.6$  lb

Damping decay results:

$\beta_1 = 0.004$ ,  $\beta_2 = 0.010$

From this table it can also be seen that modal damping generated by the circle fit routine tended to be slightly higher than that measured by free decay. This occurred because of the presence of nonlinear diminishing of the damping with response amplitude. The indicated decay values were developed from five cycles of a free decay response near the same amplitude as the steady state data.

The effective weight shown in Fig. 4 demonstrates clearly the dynamics of the slosh mechanism. The effective weight at low frequency equals the sum of that for the empty tank, rigid liquid, and two slosh masses, as indicated by Eq. (12a). At

each respective resonance the weight of each slosh mass is significantly amplified, as indicated by Eq. (14a). Finally, at frequencies above the two modes, the slosh weights have offloaded to where only the sum of the empty tank and rigid liquid weight remains, as indicated by Eq. (13a). Similar offloading response occurs for the moment, as shown in Fig. 5.

A similar set of results is also given for the same liquid level with solid baffles installed in the tank and excitation out of plane relative to the baffles. In this case the quiescent liquid level cleared the top of the baffles by 1.0 in. From Table 2 and Figs. 6 and 7, it can be seen that corresponding frequencies are lowered only slightly, but damping is increased dramatically by the baffles, especially for the first mode. At the same time, there was a tendency for the generated model to deviate

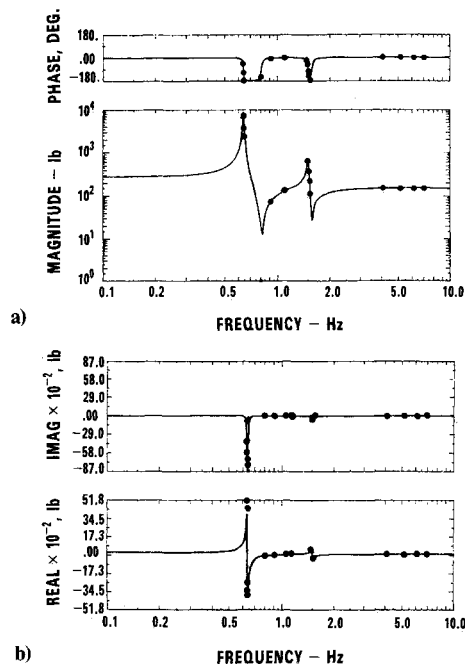


Fig. 4 Effective weight of liquid slosh for liquid level 3: a) magnitude and phase and b) real and imaginary.

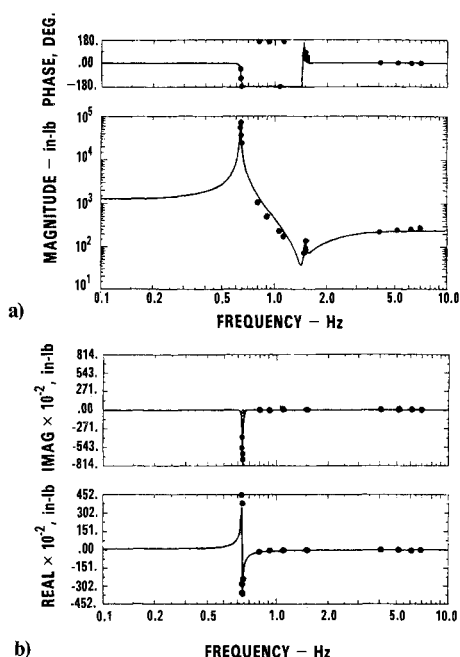


Fig. 5 Effective moment of liquid slosh for liquid level 3: a) magnitude and phase and b) real and imaginary.

Table 2 Liquid level 3 baffled tank slosh model parameters

Tank excitation level: 0.0660 in.

Slosh model parameter extraction

Input: Empty tank weight 126.24 lb

Empty tank c.g. 1.626 in

Rigid fluid weight 46.73 lb

Rigid fluid c.g. 0.463 in.

Slosh resonance data analysis mode no. 2

NPTS	$f_i$ , freq	$\beta_i$ , beta	error	$h_i$ , pivot	$m_i g$ , weight	$\ell_i$ , arm
3	1.5080	0.0086	0.0005	-0.181	18.71	4.299
5	1.5081	0.0075	0.0004	-0.174	16.93	4.299
7	1.5070	0.0085	0.0020	-0.197	20.30	4.305

Slosh resonance data analysis mode no. 1

NPTS	$f_i$ , freq	$\beta_i$ , beta	error	$h_i$ , pivot	$m_i g$ , weight	$\ell_i$ , arm
3	0.6151	0.0534	0.0000	10.090	91.36	25.841
5	0.6148	0.0529	0.0001	10.140	92.05	25.869

$\Sigma m_i g = 155$  lb, actual liquid  $W_f = 148.6$  lb

Damping decay results:

$\beta_1 = 0.044$ ,  $\beta_2 = 0.004$

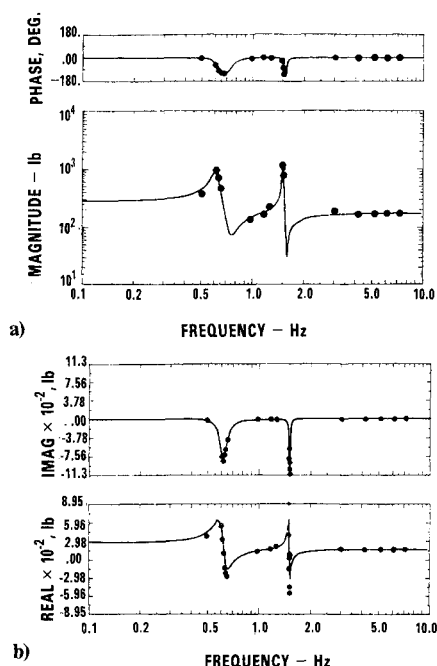


Fig. 6 Effective weight of liquid slosh for liquid level 3: a) magnitude and phase and b) real and imaginary.

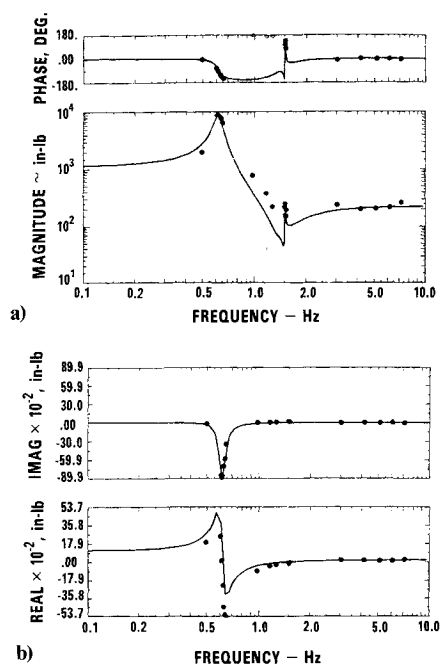


Fig. 7 Effective moment of liquid slosh for liquid level 3: a) magnitude and phase and b) real and imaginary.

from the experimental data somewhat greater than for the smooth tank. This also was caused by rather strong nonlinearity of the damping with response amplitude.

## V. Conclusions

The dynamic characterization of the liquid slosh phenomena in terms of a series of discrete pendulum oscillators is particularly well suited to the variable geometry satellite fuel tanks. Modern digital data acquisition and modal analysis procedure have been applied to the slosh model parameter extraction problem. After appropriate data conditioning to remove the tank rigid mass and liquid rigid mass from the spectral data, the slosh peaks are circle fit to obtain estimates of the slosh modal parameters. Based on results presented, which are typical of a series of results obtained thus far, the data analysis techniques proposed are quite appropriate for slosh model parameter extraction for relatively low damped as well as moderately damped tanks containing liquids.

## References

- <sup>1</sup>The *Dynamic Behavior of Liquids in Moving Containers*, edited by H.N. Abramson, NASA SP-106, 1966.
- <sup>2</sup>Sumner, I.E., Stofan, A.J., and Shamro, D.J., "Experimental Sloshing Characteristics and a Mechanical Model Analogy of Liquid Sloshing in a Scale-Model Centaur Liquid-Oxygen Tank," NASA TM X-999, 1964.
- <sup>3</sup>Dodge, F.T. and Garza, L.R., "Experimental and Theoretical Studies of Liquid Sloshing at Simulated Low Gravity," *Transactions ASME Journal of Applied Mechanics*, Vol. 34, Sept. 1967, pp. 555-561.
- <sup>4</sup>Luk, Y.W. and Mitchell, L.D., "System Identification Via Modal Analysis," ASME, Applied Mechanics Division, Vol. 59, 1983, pp. 31-49.
- <sup>5</sup>Weitzman, C., *Distributed Micro/Minicomputer Systems*, Prentice-Hall, 1980, pp. 187-191.

## From the AIAA Progress in Astronautics and Aeronautics Series

# SPACECRAFT RADIATIVE TRANSFER AND TEMPERATURE CONTROL—v. 83

Edited by T.E. Horton, The University of Mississippi

Thermophysics denotes a blend of the classical engineering sciences of heat transfer, fluid mechanics, materials, and electromagnetic theory with the microphysical sciences of solid state, physical optics, and atomic and molecular dynamics. This volume is devoted to the science and technology of spacecraft thermal control, and as such it is dominated by the topic of radiative transfer. The thermal performance of a system in space depends upon the radiative interaction between external surfaces and the external environment (space, exhaust plumes, the sun) and upon the management of energy exchange between components within the spacecraft environment. An interesting future complexity in such an exchange is represented by the recent development of the Space Shuttle and its planned use in constructing large structures (extended platforms) in space. Unlike today's enclosed-type spacecraft, these large structures will consist of open-type lattice networks involving large numbers of thermally interacting elements. These new systems will present the thermophysicist with new problems in terms of materials, their thermophysical properties, their radiative surface characteristics, questions of gradual radiative surface changes, etc. However, the greatest challenge may well lie in the area of information processing. The design and optimization of such complex systems will call not only for basic knowledge in thermophysics, but also for the effective and innovative use of computers. The papers in this volume are devoted to the topics that underlie such present and future systems.

Published in 1982, 529 pp., 6×9, illus., \$35.00 Mem., \$55.00 List

TO ORDER WRITE: Publications Dept., AIAA, 1633 Broadway, New York, N.Y. 10019